catalysts

MDPI

Article

Direct Synthesis of Dimethyl Carbonate from Methanol and CO_2 over ZrO_2 Catalysts Combined with a Dehydrating Agent and a Cocatalyst

Dichao Shi [1], Svetlana Heyte [2], Mickaël Capron [2] and Sébastien Paul [2,*]

[1] School of Chemical and Environmental Engineering, Liaoning University of Technology, Jinzhou 121001, China; shidichao@lnut.edu.cn
[2] Univ. Lille, CNRS, Centrale Lille, Univ. Artois, UMR 8181—UCCS—Unité de Catalyse et Chimie du Solide, F-59000 Lille, France; svetlana.heyte@univ-lille.fr (S.H.); mickael.capron@univ-lille.fr (M.C.)
* Correspondence: sebastien.paul@centralelille.fr

Abstract: Zirconia nanocrystals as catalysts for the direct synthesis of dimethyl carbonate (DMC) from methanol and carbon dioxide have received significant interest recently. In this paper, three zirconia-based catalysts presenting different monoclinic and tetragonal phase contents are prepared and characterized by X-ray diffraction (XRD), N_2 adsorption–desorption, transmission electron microscopy (TEM), and temperature-programmed desorption of NH_3 and CO_2 (NH_3-TPD and CO_2-TPD). The catalytic performances of these solids are evaluated in terms of DMC production. This production is low when using the bare zirconias, but it is significantly increased in the presence of 1,1,1-trimethoxymethane (TMM) playing the role of a dehydrating agent, which shifts the thermodynamic equilibrium. Moreover, the production of DMC is further improved by adding a second solid catalyst (cocatalyst), the molecular sieve 13X, to accelerate the hydration of TMM. Hence, the molecular sieve 13X plays a dual role by trapping water molecules formed by the reaction of DMC synthesis and providing strong acidic sites catalyzing TMM hydrolysis. To the best of our knowledge, the combination of two solid catalysts in the reaction medium to accelerate the water elimination to obtain higher DMC production from CO_2 and methanol has never been reported.

Keywords: zirconia nanocrystals; dimethyl carbonate; TMM; second solid catalyst

Citation: Shi, D.; Heyte, S.; Capron, M.; Paul, S. Direct Synthesis of Dimethyl Carbonate from Methanol and CO_2 over ZrO_2 Catalysts Combined with a Dehydrating Agent and a Cocatalyst. *Catalysts* **2024**, *14*, 657. https://doi.org/10.3390/catal14100657

Academic Editor: Jaime Soler

Received: 21 August 2024
Revised: 20 September 2024
Accepted: 23 September 2024
Published: 24 September 2024

1. Introduction

A significant increase in CO_2 emissions caused by the intensive consumption of coal, oil, and gas has led to a dramatic environmental issue, the so-called global warming [1–4]. Therefore, efficient measures must be taken to significantly reduce CO_2 emissions by trapping it and valorizing it into useful materials. Dimethyl carbonate (DMC) has been given much attention because it can be used as a gasoline and diesel additive [5,6] or as an ideal solvent for lithium-ion batteries [7]. In addition, the usage of DMC as a green reagent for the replacement of toxic and hazardous chemicals, such as dimethyl sulfate, phosgene ($COCl_2$), and acetate esters, is also a potential application because of its low toxicity, low viscosity, and good dissolving ability [8,9]. Hence, the development of an environmentally benign and human-friendly route for DMC synthesis using CO_2 as feedstock is essential. Direct synthesis of DMC from CO_2 and methanol drew much attention recently because of its compliance with the concept of Green Chemistry in terms of the abundance of the feedstock CO_2, production of valuable chemical DMC, and absence of toxicity.

However, there are two main drawbacks to the direct synthesis of DMC from CO_2 and methanol. CO_2 is a very stable compound ($\Delta G^0_{25\,^\circ C} = -396$ kJ/mol) that requires a high amount of energy input to be activated [10]. Various heterogeneous catalysts have been reported to decrease the energy barrier that must be overpassed to convert CO_2 to DMC, such as $H_3PMo_{12}O_{40}$ [11], $CuCl_2$/AC [12], Cu-Ni/Graphite [13], CeO_2 [14–17], and

ZrO_2 [18–20]. Among them, ZrO_2 nanocrystals showed a promising potential due to their acid–base properties [21]. ZrO_2 exhibits three polymorphs: monoclinic (*m*-ZrO_2), tetragonal (*t*-ZrO_2), and cubic (*c*-ZrO_2). The amount of acid–base sites for different polymorphs of ZrO_2 decreases in the order of *t*-ZrO_2 > *m*-ZrO_2 > *c*-ZrO_2 [18]. Tomishige et al. have demonstrated in their early study that, under 50 bar of CO_2 at 170 °C, a ZrO_2-based catalyst containing a major part of the monoclinic phase and a minor part of the tetragonal phase on its surface exhibited some DMC production (0.6 mmol/$g_{cat.}$), whereas a pure monoclinic phase was inactive [19,20]. In this work, ZrO_2 nanocrystals were prepared, varying the ratios between the monoclinic and the tetragonal phases to examine the effect on DMC production from CO_2 and methanol.

A strong limitation encountered for the direct synthesis of DMC from CO_2 and methanol is the thermodynamic equilibrium. Whatever the catalyst used, the production of DMC is far from satisfactory because the reaction is always limited. One way to obtain a higher production of DMC is to add an efficient dehydration agent in the reaction medium to shift the equilibrium by eliminating in situ the water molecules formed by the reaction. Several dehydration agents have been employed to promote the formation of DMC, such as molecular sieve 3A/4A/5A/13X [22,23], ionic liquids (ILs) [24], butylene oxide (BO) [25,26], 2,2-dimethoxypropane (DMP) [27,28], 1,1,1-trimethoxymethane (TMM) [29,30], and 2-cyanopyridine (2-CP) [31–33]. Among them, 2-CP allowed to reach excellent catalytic performances, namely 92% of methanol conversion with higher than 99% selectivity to DMC, when using CeO_2 as a catalyst under 30 bar of CO_2 at 120 °C [34]. Nevertheless, the main drawback of using 2-CP as a dehydration agent is the hazardous character of this molecule and, hence, the difficulty of operation, which limits its application in industry. BO is not a better choice as it may present complex secondary and/or tertiary reactions [25]. DMP and TMM are potential green alternatives that have been commonly used due to their relatively high reactivity with water and less production of byproducts [29,35,36]. Tomishige and co-workers showed that the DMC production was 13.8 mmol/$g_{cat.}$ over CeO_2-ZrO_2 catalyst used in combination with DMP under 60 bar of CO_2 at 110 °C, which was almost 10 times higher than that observed without a dehydration agent (1.5 mmol/$g_{cat.}$) [37]. Xuan et al. presented a much higher DMC production (6.6 mmol/$g_{cat.}$) over MOF-808-4 with TMM as a dehydration agent under 120 bar of CO_2 at 140 °C compared with that observed without adding TMM as dehydrate (0.24 mmol/$g_{cat.}$) [30]. It should be noted that, to the best of our knowledge, no publication reported the DMC synthesis from CO_2 and methanol over a bare ZrO_2 catalyst combined with DMP or TMM as dehydration agents.

Interestingly, Choi et al. found that by adding a second homogeneous catalyst, namely [Ph_2NH_2]OTf, the DMC production reached up to 40 mmol/$g_{cat.}$ over the Bu_2SnO catalyst in the presence of DMP, which was much higher than that observed without adding a second catalyst (namely 17 mmol/$g_{cat.}$) [38]. The principle of adding a second acid catalyst (called cocatalyst in the following) is to accelerate the reaction of hydration of DMP. It should be noted that traditional Brönsted acids such as HCl, H_2SO_4, and H_3PO_4 have no remarkable promotion to DMC production. Moreover, they cannot be easily separated from the medium after the reaction. Therefore, it would be interesting to identify solid cocatalysts with acidic properties able to accelerate efficiently the DMP production or the TMM hydration reaction.

Herein, ZrO_2 nanocrystals with different monoclinic and tetragonal phase contents were prepared, and their catalytic activity for the synthesis of DMC from CO_2 and methanol was investigated in the presence of a dehydration agent (TMM). Adsorption of NH_3 and CO_2 on the surface of the tested catalysts varies with monoclinic and tetragonal phase contents, showing the variety of acid–base properties, which are shown to be crucial to determining the level of production of DMC. Additionally, a solid cocatalyst (13X) was introduced in the reaction medium to promote the formation of DMC further by accelerating the hydration of TMM. Finally, 61 mmol/$g_{cat.}$ of DMC production was achieved on the ZrO_2 catalyst in the presence of TMM with adding molecular sieve 13X as a second catalyst.

2. Results and Discussion

2.1. Characterization of ZrO_2 Nanocrystals

The crystal structure of the three zirconia catalysts presenting a mixture of tetragonal and monoclinic phases in various ratios was characterized by XRD, as shown in Figure 1. Intensive diffraction peaks at 2θ = 34.6°, 35.2°, 50.2°, 59.3°, and 60.0° in Figure 1a are assigned to the tetragonal phase (PDF 01-081-1544), but they overlap with the diffraction peaks at 2θ = 34.1°, 34.4°, 35.3°, 49.4°, 50.2°, 50.5°, and 59.8° in Figure 1b,c that are assigned to the monoclinic phase (PDF 00-065-0728), thereby making clear identification of the two phases rather difficult. The quantification of both phases was conducted using the diffraction peak at 2θ = 30.2°, which can be assigned to the tetragonal phase, whereas the monoclinic phase has three distinct peaks at 2θ = 24.0°, 28.2°, and 31.5°. An intensive diffraction peak at 2θ = 30.2° appears with a very small shoulder at 2θ = 28.2° for the ZrO_2-1 catalyst, indicating the formation of a well-crystalized ZrO_2 that contains a phase mixture presenting a majority of tetragonal phase and a minority of monoclinic phase. The ZrO_2-2 catalyst presents two diffraction peaks at 2θ = 28.2° and 31.5° with a tiny peak at 2θ = 28.2° in between, meaning that the content of the monoclinic phase is much higher than that of the tetragonal phase. The intensity of the diffraction peaks at 2θ = 28.2° and 31.5° is found attenuated for the ZrO_2-3 catalyst, while the peak at 2θ = 28.2° becomes more intense in comparison with the ZrO_2-2 catalyst. It demonstrates that the content of the monoclinic phase decreases, whereas the content of the tetragonal phase increases for ZrO_2-3 compared to the ZrO_2-2 catalyst.

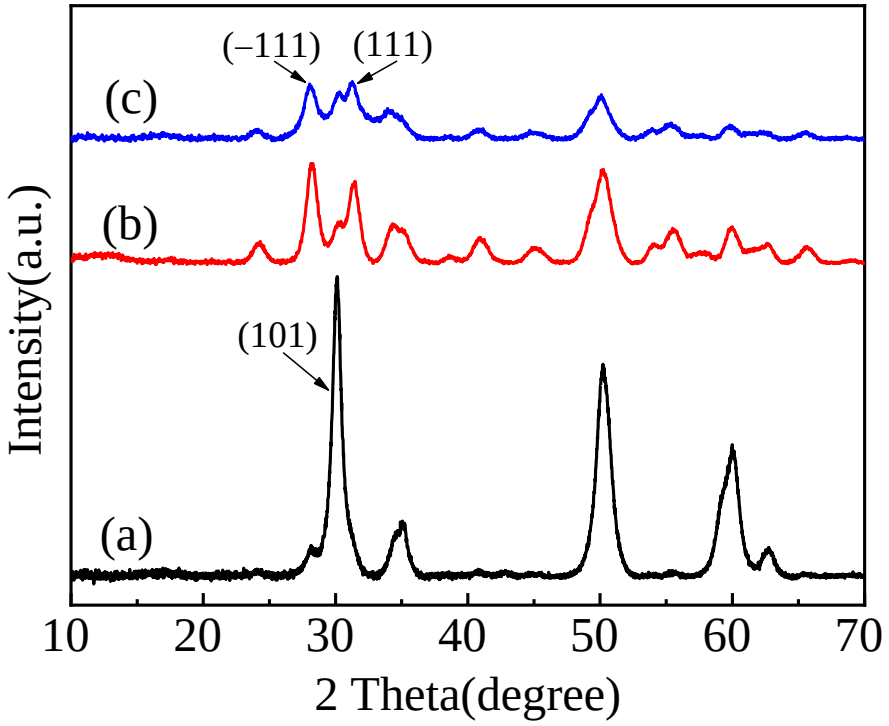

Figure 1. XRD patterns of ZrO_2-1 (**a**), ZrO_2-2 (**b**), and ZrO_2-3 (**c**).

Rietveld refinement was carried out for ZrO_2-1, ZrO_2-2, and ZrO_2-3 to determine their phase contents and lattice parameters, as shown in Table 1. According to the refinement, the ratio between the monoclinic and the tetragonal phases is 3%/97% for ZrO_2-1, 69%/31% for ZrO_2-2, and 64%/36% for ZrO_2-3.

The porous structures of the three synthesized ZrO_2 were determined from N_2 adsorption–desorption isotherms and pore size distributions, as presented in Figure 2. The adsorption–desorption isotherms are identified as type IV for the three catalysts, which is characteristic of mesoporous materials [39,40]. The hysteresis loops for samples ZrO_2-1

and ZrO_2-2 are of H_2-type, typically indicating a mesoporous pore network. The absence of a plateau at high P/P_0 for ZrO_2-3 can be described by an H4-type hysteresis, which is associated with narrow slit-like pores [41,42]. The pore size distribution obtained from the isotherms gives a single peak at 4 nm for ZrO_2-1, at 5.6 nm for ZrO_2-2, and at 4.5 nm for ZrO_2-3. The highest BET surface area is obtained for ZrO_2-3 (223 m^2/g), whereas it is 115 m^2/g for ZrO_2-1 and 101 m^2/g for ZrO_2-2.

Table 1. Rietveld refinement results for ZrO_2-1, ZrO_2-2 and ZrO_2-3.

Catalysts	Phase	Lattice Parameters	Interfacial Angle (°)	Ionic Position and Coordinate			
				Atoms	x	y	z
ZrO_2-1	Tetragonal	a = 3.62440 b = 3.62440 c = 5.15600	α = β = γ = 90	Zr O	0.75000 0.25000	0.25000 0.25000	0.75000 0.04462
	Monoclinic	a = 5.14500 b = 5.20750 c = 5.31070	α = 90 β = 99.23 γ = 90	Zr O1 O2	0.27831 0.19088 0.42585	0.00025 0.49701 0.88364	0.20448 0.13474 0.36247
ZrO_2-2	Tetragonal	a = 3.62440 b = 3.62440 c = 5.15600	α = β = γ = 90	Zr O	0.75000 0.25000	0.25000 0.25000	0.75000 0.00345
	Monoclinic	a = 5.14500 b = 5.20750 c = 5.31070	α = 90 β = 99.23 γ = 90	Zr O1 O2	0.28329 0.06090 0.39521	0.04115 0.33632 0.73584	0.21327 0.34648 0.47151
ZrO_2-3	Tetragonal	a = 3.62440 b = 3.62440 c = 5.15600	α = β = γ = 90	Zr O	0.75000 0.25000	0.25000 0.25000	0.75000 0.03912
	Monoclinic	a = 5.14500 b = 5.20750 c = 5.31070	α = 90 β = 99.23 γ = 90	Zr O1 O2	0.27732 0.07258 0.41583	0.03893 0.34447 0.74603	0.21013 0.34290 0.48318

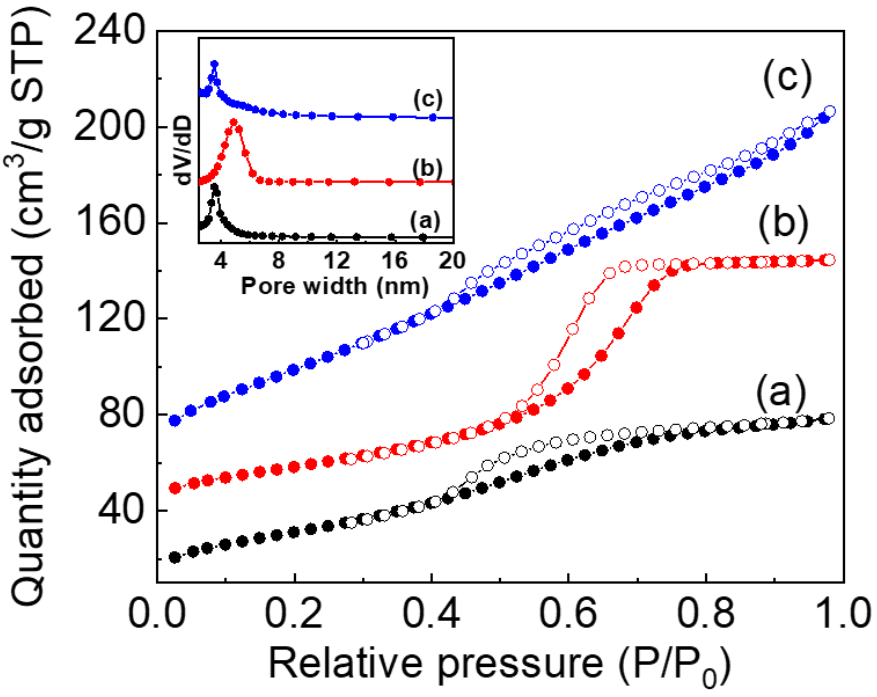

Figure 2. Nitrogen adsorption–desorption isotherms of ZrO_2-1 (**a**), ZrO_2-2 (**b**), and ZrO_2-3 (**c**). The insert shows the pore size distributions.

Crystal sizes of all ZrO_2 catalysts were investigated by TEM and HRTEM, as shown in Figure 3. TEM images of ZrO_2-1 (Figure 3a) and ZrO_2-2 (Figure 3c) show that the particle sizes are in the range of 10–15 nm in all cases and the particles present a strong aggregation. The interplanar spacing of the mainly exposed planes is 0.3 nm, corresponding to (101) planes of the tetragonal phase for ZrO_2-1 (Figure 3b), and 0.32 nm corresponding to (−111) planes of the monoclinic phase for ZrO_2-2 (Figure 3d), implying that ZrO_2-1 is a tetragonal phase-rich crystal, whereas ZrO_2-2 is a monoclinic phase-rich crystal. This result is in good agreement with the conclusion made according to XRD patterns. However, the ZrO_2-3 sample shows less aggregation and presents a smaller particle size (8–10 nm, Figure 3e) in comparison with the other two samples. This is also consistent with the higher surface area of ZrO_2-3 as compared with those of ZrO_2-1 and ZrO_2-2. In addition, the presence of interplanar spacing of 0.3 nm and 0.32 nm, which are attributed to the (101) and (−111) planes of the tetragonal phase and the monoclinic phase, respectively (Figure 3f), implies that ZrO_2-3 contains more tetragonal phase compared to ZrO_2-2.

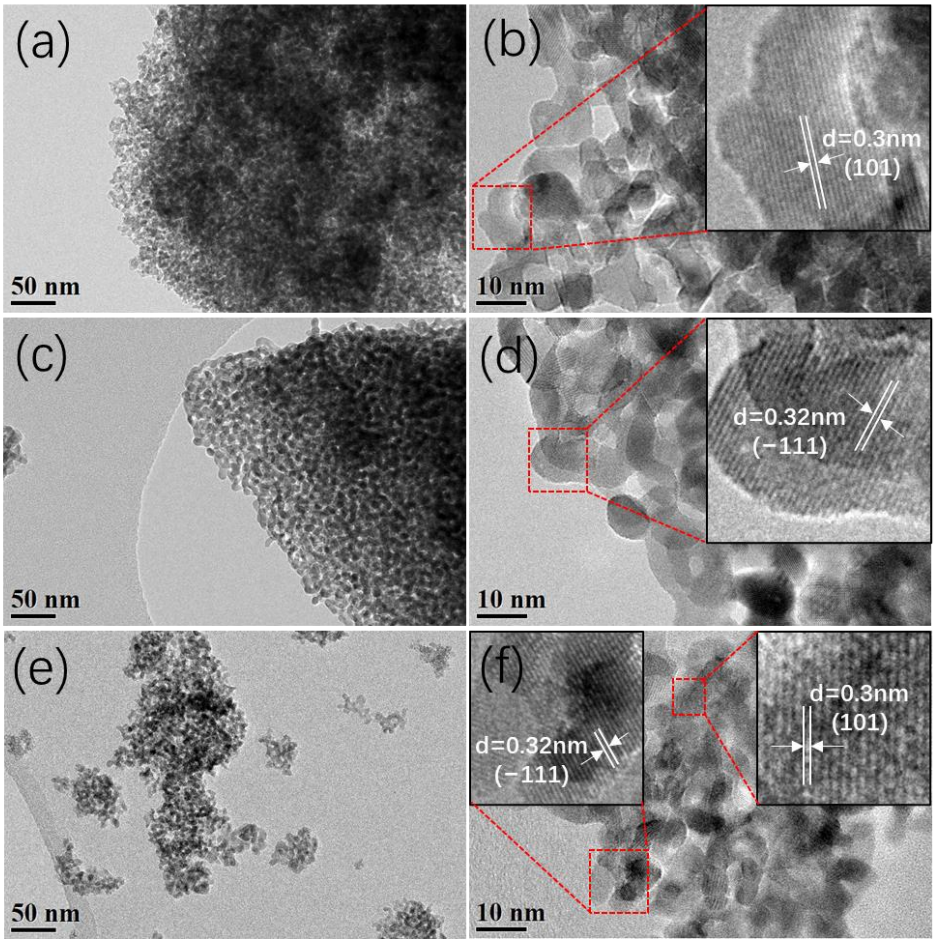

Figure 3. TEM and HRTEM images of ZrO_2-1 (**a**,**b**), ZrO_2-2 (**c**,**d**), and ZrO_2-3 (**e**,**f**).

It is known that the amounts of acidic and basic sites are crucial to the formation of DMC from CO_2 and methanol [14]. Therefore, NH_3-TPD and CO_2-TPD measurements were used to investigate the acid–base properties of zirconia nanocrystals. The desorption peaks with peak maximum located at <200 °C, 200–400 °C, and >400 °C are attributed to weak, moderate, and strong acidic/basic sites, respectively, as summarized in Table 2. The total amounts of NH_3/CO_2 desorbed from acid/base sites increased in the order: ZrO_2-3 > ZrO_2-2 > ZrO_2-1. It should be noted that the total amounts of desorbed NH_3/CO_2 are mainly derived from moderate and strong acidic/basic sites. The ZrO_2-1 sample, which mainly contains a tetragonal phase, presents stronger acid sites, while ZrO_2-2, containing mainly

a monoclinic phase, has more moderate acid sites. On the contrary, the ZrO_2-1 sample contains more moderate basic sites, whereas ZrO_2-2 has stronger basic sites. However, the ZrO_2-3 sample, which contains certain contents of the tetragonal phase and monoclinic phase, presents the highest total amounts of moderate and strong acidic/basic sites as compared to the other two samples. The high total amount of acidic/basic sites for ZrO_2-3 may be due to its contents of the tetragonal phase and monoclinic phase, as well as its high surface area. This is consistent with the results reported previously in the literature [19].

Table 2. Acidic and basic amounts of ZrO_2 catalysts were determined from NH_3-TPD and CO_2-TPD measurements.

Samples	NH_3 Absorption (μmol/g) [a]				CO_2 Absorption (μmol/g) [b]			
	Weak (<200 °C)	Moderate (200–400 °C)	Strong (>400 °C)	Total	Weak (<200 °C)	Moderate (200–400 °C)	Strong (>400 °C)	Total
ZrO_2-1	5	68	87	160	0	70	50	120
ZrO_2-2	21	168	81	270	24	63	103	190
ZrO_2-3	2	162	186	350	39	149	182	370

[a] As determined from NH_3-TPD measurement. [b] As determined from CO_2-TPD measurement.

2.2. Catalytic Performance of ZrO_2 Nanocrystals

The catalytic performances of zirconia nanocrystals were examined for the direct synthesis of DMC from methanol and CO_2. In order to identify the optimal reaction temperature for a high DMC production, different reaction temperatures have been used to evaluate the catalytic activity of the ZrO_2-3 catalyst, as shown in Figure 4. DMC production increased dramatically with the reaction temperature to reach 0.2 mmol/$g_{cat.}$ at 130 °C. It decreased slightly when further increasing the reaction temperature. This may be explained by the preferential formation of dimethyl ether (DME) at high reaction temperatures [43]. Therefore, a reaction temperature of 130 °C turned out to be optimal and was kept for the rest of the study.

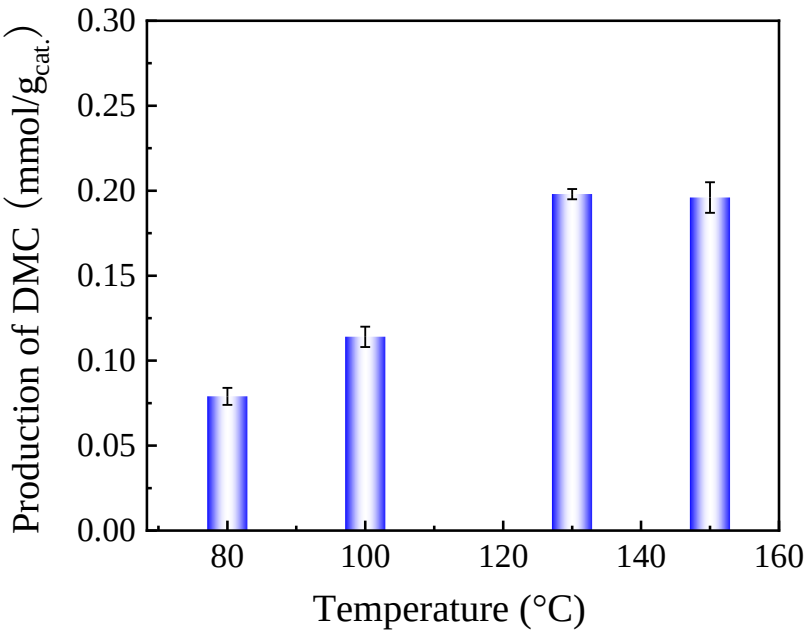

Figure 4. DMC production as a function of the reaction temperature on the ZrO_2-3 catalyst. Reaction conditions: 2 mL of methanol, 30 mg of catalyst, 38 bar CO_2 pressure, 6 h reaction time. The error bars correspond to the standard deviation from three independent measurements.

Figure 5 depicts that the three zirconia catalysts exhibited different catalytic performances (blue bars) in the order of ZrO_2-3 > ZrO_2-2 > ZrO_2-1, which is consistent with the amounts of acidic and basic sites measured for each catalyst. The ZrO_2-3 catalyst shows the best DMC production as compared to the other two catalysts. However, the performances are still very low. Finding an efficient dehydrating agent that could react with water formed by the reaction and hence shift the thermodynamic equilibrium and promote DMC production is therefore necessary.

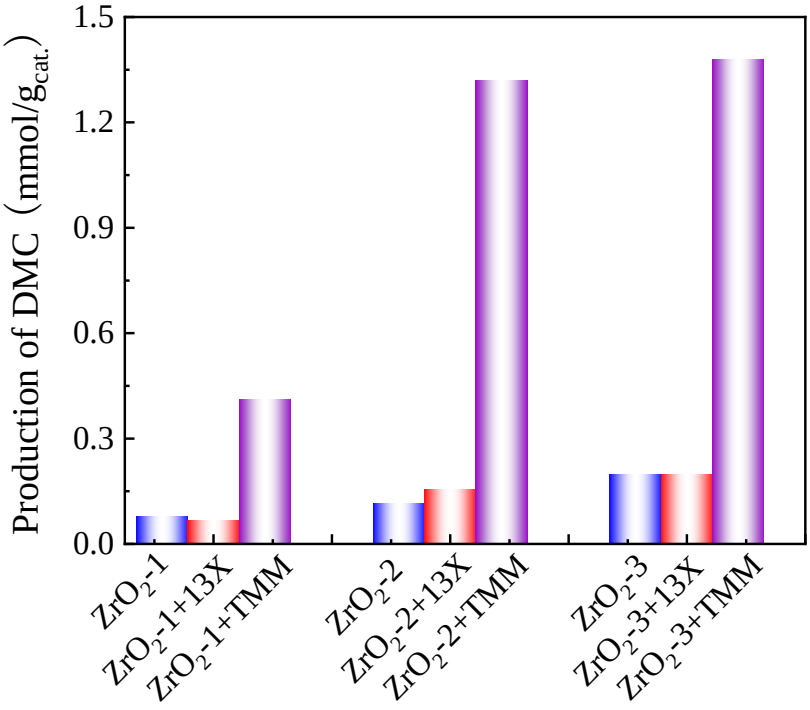

Figure 5. DMC production on three zirconia-based catalysts (blue bars), in the presence or absence of 13X (red bars) and TMM as dehydration agent (violet bars). Reaction conditions: 2 mL of methanol for the reactors with zirconia as catalyst and for the reactors with zirconia as catalysts in combination with 13X, 1 mL of methanol for the reactors with zirconia as catalyst in combination with TMM, 1.3 mL of TMM (molar ratio methanol/TMM is 2:1) if present, 30 mg of catalyst, 150 mg of 13X if present, under 38 bar CO_2 pressure, 130 °C, and 6 h reaction time.

Molecular sieves have been widely reported as inorganic dehydration agents for the formation of DMC from CO_2 and methanol due to the advantages of easy operation, no byproduct formation, and recyclability [27,44]. In our study, molecular sieve 13X was tested alone and in combination with TMM, but no DMC was produced. When molecular sieve 13X was combined with zirconia as a catalyst (as shown in Figure 5 red bars), it did not present any promotion of DMC production. However, it did not degrade DMC either. TMM was then tested as a dehydrating agent. It is of particular interest to note that when TMM reacts with water, it forms methanol, which is one of the main reactants. It turned out that TMM is a very efficient dehydrating agent to promote DMC production when combined with all three zirconia catalysts (violet bars), suggesting that TMM has a relatively high reactivity with water. Specifically, for the ZrO_2-3 catalyst, the DMC production reaches up to 1.4 mmol/$g_{cat.}$, showing that TMM is a suitable dehydration agent for the synthesis of DMC.

To further increase the DMC production, the effect of reaction time was investigated for the three zirconia catalysts (Figure 6). The DMC production increased remarkably on all three zirconia catalysts, with increasing the reaction time when combined with TMM as a dehydration agent. ZrO_2-3 catalyst exhibited a 24 mmol/$g_{cat.}$ DMC production after 48 h of

reaction, which is 17 times higher than after 6 h of reaction. The DMC production after 48 h on the ZrO_2-3 catalyst is significantly higher than that on the ZrO_2-1 and ZrO_2-2 catalysts.

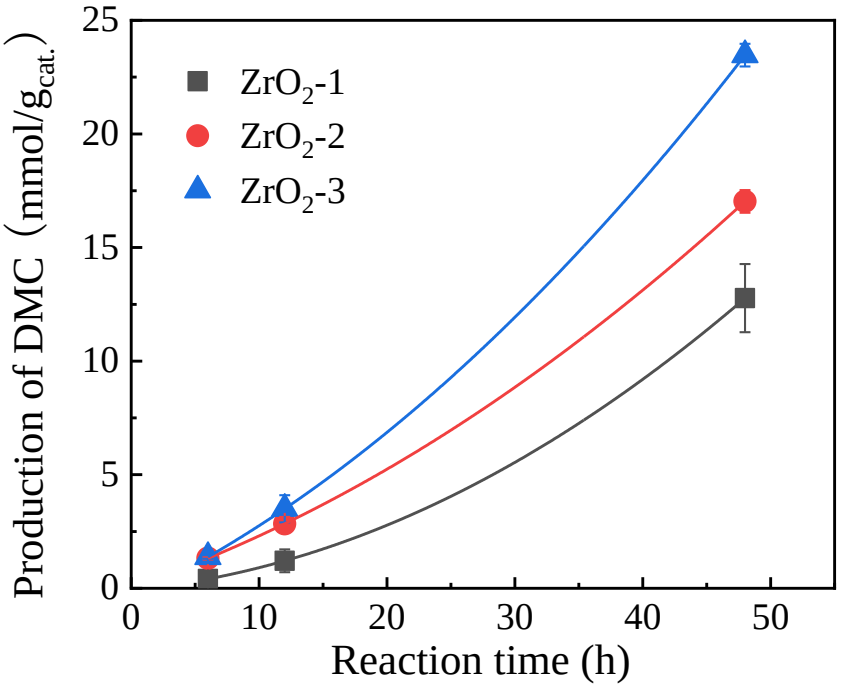

Figure 6. Effect of reaction time on the production of DMC on different types of zirconia catalysts with TMM as dehydration agent. Reaction conditions: 1 mL of methanol, 1.3 mL of TMM (molar ratio methanol/TMM is 2:1), 30 mg of zirconia, under a 38 bar CO_2 pressure, at 130 °C reaction temperature, with 6 h, 12 h, and 48 h reaction times. The error bars correspond to the standard deviation calculated from three independent measurements.

However, even if the ZrO_2-3 catalyst presents a high DMC production after 48 h of reaction with TMM as a dehydration agent, a lot of TMM remains in the medium (conversion of TMM is only 31% after 48 h). Therefore, adding a second catalyst in the medium (cocatalyst) to promote the hydration of TMM is proposed to accelerate what is believed to be the limiting step of the whole process. The difficulty of selecting a cocatalyst is to avoid the degradation of DMC while accelerating the hydration of TMM. It has been reported that TMM can easily be hydrolyzed in the presence of strong acidic sites [45–47]. Hence, solid catalysts with strong acid sites should be first tested. Molecular sieve 13X, which was investigated as a dehydration agent in our work, came to our mind because of its water adsorption capacity and strong acidic properties [48–50]. Moreover, 13X is available on a commercially large scale [51].

Figure 7 shows that the DMC production improved to a certain extent with increasing the mass of the second catalyst, 13X, on the ZrO_2-3 catalyst with TMM as a dehydration agent. A total of 30 mg of the cocatalyst presents the highest catalytic performances after 6 h of reaction. DMC production decreases when more cocatalyst is added, even if the conversion of TMM continues to increase linearly. It is believed that DMC is decomposed by a too large number of acidic sites introduced by supplementary 13X [52]. In our reaction, 30 mg of the second catalyst has been chosen for the rest of the study. It has to be noted that 13X has a dual role, as it can also trap water during the reaction. To the best of our knowledge, the combination of two solid catalysts in the reaction medium to accelerate in situ water elimination and obtain high DMC production has never been reported.

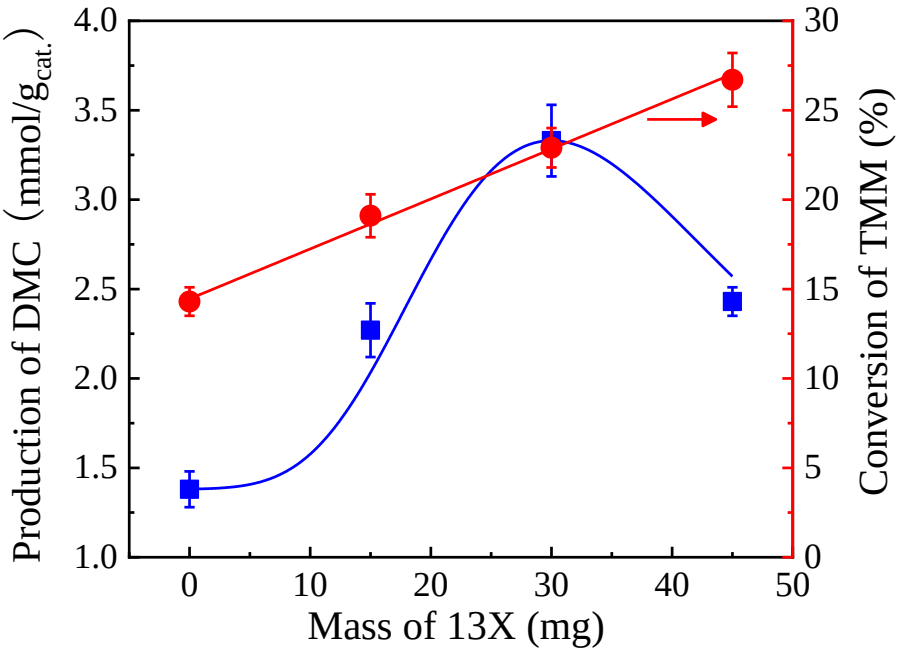

Figure 7. Production of DMC (blue squares) and TMM (red dots) conversion as a function of the mass of 13X added to the ZrO_2-3 catalyst using TMM as a dehydrating agent. Reaction conditions: 1 mL of methanol, 1.3 mL of TMM (molar ratio methanol/TMM is 2:1), 30 mg of catalyst, 38 bar CO_2 pressure, 130 °C, 6 h reaction time. The error bars correspond to the standard deviation calculated from three independent measurements.

The effect of the methanol/TMM molar ratio on the DMC production on ZrO_2-3 with the addition of 13X as cocatalyst has also been investigated by varying the volume of TMM added in a fixed volume of methanol solution (1 mL). It should be noted that even if a stoichiometric molar ratio of methanol and TMM of 2:1 is used, the TMM is not completely consumed at the end of the reaction, even when 13X is added as a second catalyst to promote hydration. DMC production decreased dramatically when reducing the TMM amount in the reaction medium, and finally, it reached a plateau when the molar ratio of methanol and TMM was 6:1, as shown in Figure 8. Therefore, the stoichiometric ratio of methanol and TMM is optimal and used in the following of the study, even if it has to be noted here that the presence of unconverted TMM in the reactive medium after the reaction is not desired as it must be separated from DMC by distillation, which is an energy-intensive separation method.

The influence of the reaction time on DMC production was studied in the presence of a ZrO_2-3 catalyst using 13X as a cocatalyst and TMM as a dehydration agent, as shown in Figure 9. DMC production increased remarkably with prolonged reaction time, and it arrived at a high value of 61 mmol/$g_{cat.}$ after 48 h of reaction, which is more than 2.5 times more than without adding 13X as a cocatalyst (see Figure 6). DMC production is therefore significantly improved on the ZrO_2-3 catalyst by adding 13X as a cocatalyst to promote the hydrolysis of TMM used as a dehydration agent.

Table 3 shows a comparison of the catalytic performances of our best catalysts (ZrO_2-3) with other Zr-based catalysts used in the literature for the direct synthesis of DMC from CO_2 and methanol. The production of DMC obtained in this work is significantly higher than the previous reports, indicating the efficiency of the solid cocatalyst approach.

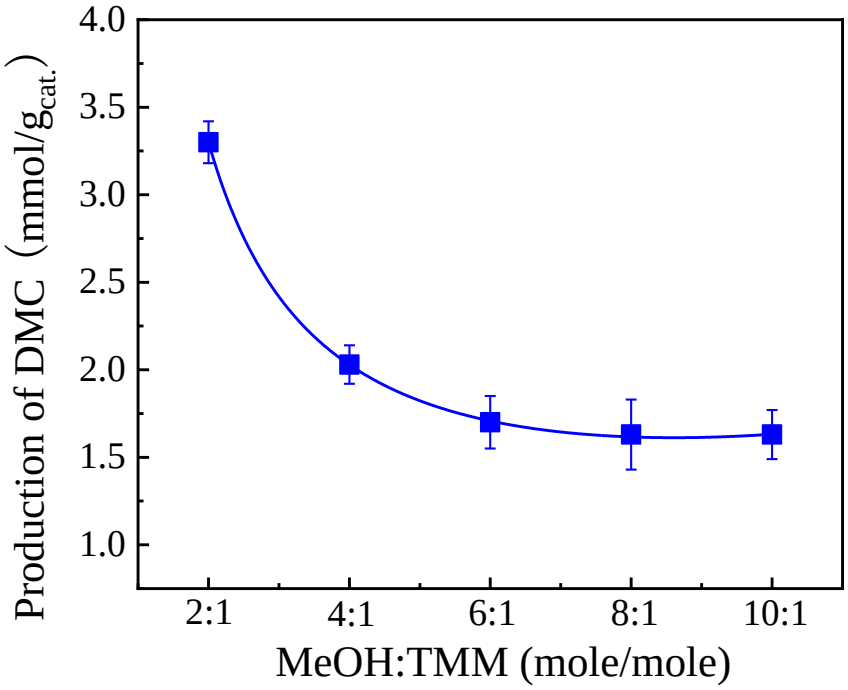

Figure 8. Effect of the methanol/TMM molar ratio on the DMC production using ZrO_2-3 catalyst and 13X as second catalyst. Reaction conditions: 1 mL of methanol, 30 mg of zirconia, 30 mg of 13X, 38 bar CO_2 pressure, 130 °C, and 6 h reaction time. The error bars correspond to the standard deviation calculated from three independent measurements.

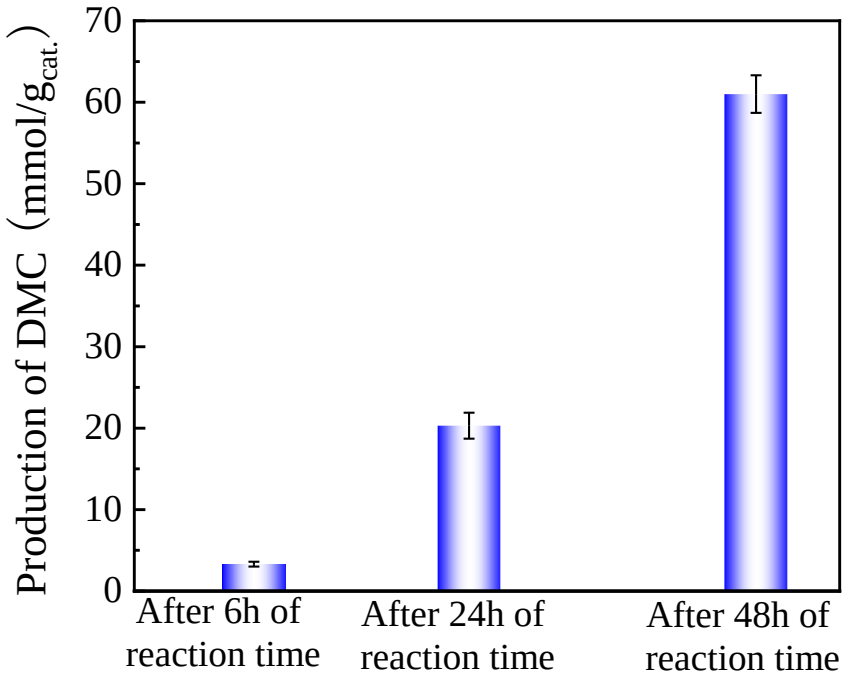

Figure 9. Effect of reaction time on the production of DMC using ZrO_2-3 catalyst with 13X as second catalyst and TMM as dehydration agent. Reaction conditions: 1 mL of methanol, 1.3 mL of TMM (molar ratio methanol/TMM is 2:1), 30 mg of zirconia ZrO_2-3, 30 mg of 13X, 38 bar CO_2 pressure, 130 °C, and 6 h, 24 h, and 48 h of reaction times. The error bars correspond to the standard deviation calculated from three independent measurements.

Table 3. Comparison of the catalytic performances of ceria-based catalysts using organic dehydration agents.

Entry	Catalyst	Dehydration Agent	Temp. (°C)	Time (h)	DMC Production ($mmol/g_{cat.}$)	Ref.
1	ZrO_2	-	160	16	10.5	[20]
2	$Ce_{0.1}Zr_{0.9}O_2$	MS 3A	170	70	6.2	[22]
3	CeO_2-ZrO_2	DMP	110	140	13.8	[37]
4	$Ce_{0.5}Zr_{0.5}O_2$	DMP	140	3	23.6	[39]
5	ZrO_2	TMM	130	48	61	This work

3. Materials and Methods

3.1. Materials

Zirconium carbonate, nitric acid (70%), ammonia solution (28%), methanol (≥99.8%), 2,2-dimethoxypropane (98%), and trimethyl orthoformate (also called 1,1,1-trimethoxymethane for synthesis) were all purchased from Sigma Aldrich (St. Louis, MO, USA) and used as received. CO_2 (99.9%) used as a reagent for the reaction was supplied by Air Liquide (Paris, France). A molecular sieve 13X (100–120 mesh, abbreviated as 13X in this paper) was supplied by Chromoptic (Villejust, France).

3.2. Synthesis of ZrO_2 Nanocrystals

A 4.6 M solution of zirconium nitrate was formulated by dissolving 1 kg of zirconium carbonate into nitric acid (HNO_3). Zirconium nitrate solution was subsequently added to 1.5 L of ammonia solution ($NH_3 \cdot H_2O$) at a rate of 10 mL/min with constant stirring to precipitate. The resulting precipitate was allowed to age within the mother liquor for durations of 48 h, 24 h, or no aging (0 h) at a constant temperature. Following the designated aging period, the precipitate underwent multiple washes before being dried overnight at 120 °C in an oven. All synthesized samples were subjected to calcination at 400 °C for 2 h in a static air atmosphere with a heating rate of 5 °C/min, followed by cooling to room temperature inside the oven. In this study, the sample aged for 48 h was denoted as ZrO_2-1, the sample aged for 24 h as ZrO_2-2, and the sample with no aging (0 h) as ZrO_2-3.

3.3. Characterization

X-ray diffraction patterns (XRD) were recorded in ambient conditions using the Cu Kα radiation (λ = 1.5418 Å; 40 kV, 30 mA) on a D8 Discovery diffractometer from Bruker AXS GmbH (Karlsruhe, Germany) equipped with Siemens X-ray tube. The 2θ of the wide angle ranged from 10° to 70°. The N_2 adsorption–desorption measurement was carried out using nitrogen adsorption at liquid-nitrogen temperature (77 K). The sample was degassed at 75 °C for 1 h and at 130 °C for 2 h. The specific surface area was evaluated with the Brunauer–Emmett–Teller (BET) model, and the pore size distribution was measured with the Barrett–Joyner–Halenda (BJH) model over the range P/P_0 = 0.05–0.30. The total pore volume was measured from the volume of N_2 adsorbed at P/P_0 = 0.95. Temperature-programmed desorption of NH_3 and CO_2 (NH_3-TPD and CO_2-TPD) was performed to quantify the amount and strength of the acid–base sites of the catalysts. A typical test was as follows: 50 mg catalysts were pre-treated in a He flow (30 mL/min) at 130 °C for 2 h in order to remove the physisorbed water. Then, NH_3 (CO_2) was absorbed at the surface by pulsed injections at 130 °C until saturation was stated from the MS signal. The TPD profiles were monitored by MS and thermal conductivity detector and recorded from 130 to 650 °C at a heating rate of 10 °C/min. Transmission electron microscopy (TEM) images were performed on a Tecnai G2 20 microscope (Waltham, MA, USA) equipped with LaB6 filament and operating at 200 kV. Samples for TEM analyses were prepared by dispersing the powder products as a slurry in ethanol and then deposited on a carbon film coated on a copper grid.

3.4. Catalytic Evaluation

The catalytic activity for the direct synthesis of DMC from CO_2 and methanol was evaluated on the REALCAT platform using a Screening Pressure Reactor (SPR) system from Unchained Labs (Pleasanton, CA, USA) equipped with 24 parallel stainless steel batch reactors of 6 mL each [53]. Typically, 30 mg of ZrO_2 nanocrystals or/and 30 mg of molecular sieve 13X were placed into the reactors with 1 mL of methanol and 1.3 mL of TMM (the molar ratio of methanol and TMM is 2:1). Before the reaction, the reactors were purged with CO_2 several times to remove air and then pressurized up to 20 bar with CO_2 at room temperature. The reaction temperature and pressure of the reactor were raised to 130 °C and 38 bar for carrying out the reaction for a given time with a continuous stirring of 700 rpm and then cooled down. Reaction products were analyzed using Shimadzu GC-2010 Plus and GC-FID-2010 Plus AF Ultra EI gas chromatographs, equipped with a FID detector (Shimadzu Corporation, Kyoto, Japan) and a ZB-WAX Plus column (30 m × 0.25 mm × 0.25 μm) (Phenomenex, Torrance, CA, USA). Solutions after the reaction were filtered to eliminate the solid and analyzed without further dilution.

4. Conclusions

In this work, three zirconia-based catalysts with different monoclinic and tetragonal phase contents were prepared and characterized. The ZrO_2-3 catalyst, presenting a mixture of monoclinic and tetragonal phases, presented the highest DMC production because of its large surface area and high total amount of acidic and basic sites. The DMC production was significantly increased by using TMM as a dehydration agent, which reacts with the water molecules formed by the reaction, hence shifting the thermodynamic equilibrium. Most importantly, this shift was further enhanced by the addition of a second solid catalyst molecular sieve, 13X, to accelerate the reaction of TMM hydrolysis. The catalytic effectiveness of the molecular sieve 13X is due to its strong acidic sites and water adsorption capacity.

At a temperature of 130 °C, a pressure of 38 bar of CO_2, a molar ratio of MeOH/TMM of 2:1, using 30 mg of ZrO_2-3 catalyst and 30 mg of 13X, 61 mmol DMC/$g_{cat.}$ could be produced after 48 h of reaction. This is 2.5 times higher than without adding 13X as a cocatalyst.

Author Contributions: Conceptualization, D.S. and S.P.; methodology, D.S. and S.H.; validation, D.S., S.H., M.C. and S.P.; formal analysis, D.S.; investigation, S.P.; resources, S.P.; data curation, D.S.; writing—original draft preparation, D.S.; writing—review and editing, S.P.; supervision, S.P.; project administration, S.P.; funding acquisition, S.P. All authors have read and agreed to the published version of the manuscript.

Funding: This research was carried out in the frame of the VULCADIME project funded by the European Community through the Eurostars 113359 (call21) program. The REALCAT platform used in this work benefits from a state subsidy administered by the French National Research Agency (ANR) within the frame of the 'Future Investments' program (PIA) with the contractual reference ANR-11-EQPX-0037.

Data Availability Statement: Data are contained within the article.

Acknowledgments: The authors thank all the partners of the project for the very fruitful discussion and collaboration. The Carbon Recycling International company is acknowledged for supplying the zirconia catalysts used in this paper. The European Union, through the ERDF funding administered by the Hauts-de-France Region, Centrale Lille, the CNRS, and Lille University, as well as the Centrale Initiatives Foundation, is thanked for their financial contributions to the acquisition and implementation of the equipment of the REALCAT platform.

Conflicts of Interest: The authors declare no conflicts of interest.

References

1. Akhundi, A.; Habibi-Yangjeh, A.; Abitorabi, M.; Rahim Pouran, S. Review on Photocatalytic Conversion of Carbon Dioxide to Value-Added Compounds and Renewable Fuels by Graphitic Carbon Nitride-Based Photocatalysts. *Catal. Rev. Sci. Eng.* **2019**, *61*, 595–628. [CrossRef]
2. Zhang, Q.; Yuan, H.Y.; Fukaya, N.; Choi, J.C. Alkali Metal Salt as Catalyst for Direct Synthesis of Carbamate from Carbon Dioxide. *ACS Sustain. Chem. Eng.* **2018**, *6*, 6675–6681. [CrossRef]
3. Sajna, M.S.; Zavahir, S.; Popelka, A.; Kasak, P.; Al-Sharshani, A.; Onwusogh, U.; Wang, M.; Park, H.; Han, D. Electrochemical System Design for CO_2 Conversion: A Comprehensive Review. *J. Environ. Chem. Eng.* **2023**, *11*, 110467–110496. [CrossRef]
4. Yan, S.; Li, W.; He, D.; He, G.; Chen, H. Recent Research Progress of Metal-organic Frameworks (MOFs) Based Catalysts for CO_2 Cycloaddition Reaction. *Mol. Catal.* **2023**, *550*, 113608–113624. [CrossRef]
5. Kumar, P.; Srivastava, V.C.; Štangar, U.L.; Mušič, B.; Mishra, I.M.; Meng, Y. Recent Progress in Dimethyl Carbonate Synthesis Using Different Feedstock and Techniques in the Presence of Heterogeneous Catalysts. *Catal. Rev. Sci. Eng.* **2019**, *63*, 363–421. [CrossRef]
6. Pawar, A.A.; Lee, D.; Chung, W.J.; Kim, H. Understanding the Synergy between MgO-CeO_2 as an Effective Promoter and Ionic Liquids for High Dimethyl Carbonate Production from CO_2 and Methanol. *Chem. Eng. J.* **2020**, *395*, 124970. [CrossRef]
7. Raza, A.; Ikram, M.; Guo, S.; Baiker, A.; Li, G. Green Synthesis of Dimethyl Carbonate from CO_2 and Methanol: New Strategies and Industrial Perspective. *Adv. Sustain. Syst.* **2022**, *6*, 2200087. [CrossRef]
8. Shi, D.; Wojcieszak, R.; Paul, S.; Marceau, E. Ni Promotion by Fe: What Benefits for Catalytic Hydrogenation? *Catalysts* **2019**, *9*, 451. [CrossRef]
9. Fiorani, G.; Perosa, A.; Selva, M. Dimethyl Carbonate: A Versatile Reagent for a Sustainable Valorization of Renewables. *Green Chem.* **2018**, *20*, 288–322. [CrossRef]
10. Zhang, S.; Xia, Z.; Zou, Y.; Cao, F.; Liu, Y.; Ma, Y.; Qu, Y. Interfacial Frustrated Lewis Pairs of CeO_2 Activate CO_2 for Selective Tandem Transformation of Olefins and CO_2 into Cyclic Carbonates. *J. Am. Chem. Soc.* **2019**, *141*, 11353–11357. [CrossRef]
11. Allaoui, L.A.; Aouissi, A. Effect of the Brønsted Acidity on the Behavior of CO_2 Methanol Reaction. *J. Mol. Catal. A Chem.* **2006**, *259*, 281–285. [CrossRef]
12. Bian, J.; Wei, X.W.; Jin, Y.R.; Wang, L.; Luan, D.C.; Guan, Z.P. Direct Synthesis of Dimethyl Carbonate over Activated Carbon Supported Cu-Based Catalysts. *Chem. Eng. J.* **2010**, *165*, 686–692. [CrossRef]
13. Bian, J.; Xiao, M.; Wang, S.J.; Lu, Y.X.; Meng, Y.Z. Novel Application of Thermally Expanded Graphite as the Support of Catalysts for Direct Synthesis of DMC from CH_3OH and CO_2. *J. Colloid Interface Sci.* **2009**, *334*, 50–57. [CrossRef] [PubMed]
14. Tian, L.; Tan, Z.; Wang, Q.; Liao, Y.-S.; Chou, J.-P.; Wu, J.-M.; Liu, G.; Peng, Y.-K. Cerium Coordination-Dependent Surface Intermediates Regulate Activity in Dimethyl Carbonate Synthesis from CO_2 and Methanol. *Appl. Catal. B Environ.* **2023**, *336*, 122914. [CrossRef]
15. Unnikrishnan, P.; Darbha, S. Direct Synthesis of Dimethyl Carbonate from CO_2 and Methanol over CeO_2 Catalysts of Different Morphologies. *J. Chem. Sci.* **2016**, *128*, 957–965. [CrossRef]
16. Huo, L.; Wang, L.; Li, J.; Pu, Y.; Xuan, K.; Qiao, C.; Yang, H. Cerium Doped Zr-Based Metal-Organic Framework as Catalyst for Direct Synthesis of Dimethyl Carbonate from CO_2 and Methanol. *J. CO2 Util.* **2023**, *68*, 102352. [CrossRef]
17. Al-Darwish, J.; Senter, M.; Lawson, S.; Rezaei, F.; Rownaghi, A.A. Ceria Nanostructured Catalysts for Conversion of Methanol and Carbon Dioxide to Dimethyl Carbonate. *Catal. Today* **2019**, *350*, 120–126. [CrossRef]
18. Wang, X.; Zhao, J.; Sun, W.; Pei, Y.; An, J.; Li, Z.; Ren, J. A DFT Study of Dimethyl Carbonate Synthesis from Methanol and CO_2 on Zirconia: Effect of Crystalline Phases. *Comput. Mater. Sci.* **2019**, *159*, 210–221. [CrossRef]
19. Tomishige, K.; Ikeda, Y.; Sakaihori, T.; Fujimoto, K. Catalytic Properties and Structure of Zirconia Catalysts for Direct Synthesis of Dimethyl Carbonate from Methanol and Carbon Dioxide. *J. Catal.* **2000**, *192*, 355–362. [CrossRef]
20. Tomishige, K.; Sakaihori, T.; Ikeda, Y.; Fujimoto, K. A Novel Method of Direct Synthesis of Dimethyl Carbonate from Methanol and Carbon Dioxide Catalyzed by Zirconia. *Catal. Lett.* **1999**, *58*, 225–229. [CrossRef]
21. Abdelhamid, H. Removal of Carbon Dioxide Using Zeolitic Imidazolate Frameworks: Adsorption and Conversion via Catalysis. *Appl. Organomet. Chem.* **2022**, *36*, 6753–6790. [CrossRef]
22. Zheng, Q.; Nishimura, R.; Sato, Y.; Inomata, H.; Ota, M.; Watanabe, M.; Camy, S. Dimethyl Carbonate (DMC) Synthesis from Methanol and Carbon Dioxide in the Presence of ZrO_2 Solid Solutions and Yield Improvement by Applying a Natural Convection Circulation System. *Chem. Eng. J.* **2022**, *429*, 132378. [CrossRef]
23. Diban, N.; Aguayo, A.T.; Bilbao, J.; Urtiaga, A.; Ortiz, I. Membrane Reactors for in Situ Water Removal: A Review of Applications. *Ind. Eng. Chem. Res.* **2013**, *52*, 10342–10354. [CrossRef]
24. Wu, R.C.; Xie, T.; Li, M. Direct Synthesis of Dimethyl Carbonate Form Methanol and Carbon Dioxide Using $H_3PW_{12}O_{40}/Ce_{0.1}Ti_{0.9}O_2$ with Ionic Liquid Catalysts. *Adv. Mater. Res.* **2012**, *418–420*, 38–41. [CrossRef]
25. Eta, V.; Mäki-Arvela, P.; Leino, A.R.; Kordás, K.; Salmi, T.; Murzin, D.Y.; Mikkola, J.P. Synthesis of Dimethyl Carbonate from Methanol and Carbon Dioxide: Circumventing Thermodynamic Limitations. *Ind. Eng. Chem. Res.* **2010**, *49*, 9609–9617. [CrossRef]
26. Eta, V.; Mäki-Arvela, P.; Salminen, E.; Salmi, T.; Murzin, D.Y.; Mikkola, J.P. The Effect of Alkoxide Ionic Liquids on the Synthesis of Dimethyl Carbonate from CO_2 and Methanol over ZrO_2-MgO. *Catal. Lett.* **2011**, *141*, 1254–1261. [CrossRef]

27. Honda, M.; Tamura, M.; Nakagawa, Y.; Nakao, K.; Suzuki, K.; Tomishige, K. Organic Carbonate Synthesis from CO_2 and Alcohol over CeO_2 with 2-Cyanopyridine: Scope and Mechanistic Studies. *J. Catal.* **2014**, *318*, 95–107. [CrossRef]
28. Nanda, M.R.; Zhang, Y.; Yuan, Z.; Qin, W.; Ghaziaskar, H.S.; Xu, C. Catalytic Conversion of Glycerol for Sustainable Production of Solketal as a Fuel Additive: A Review. *Renew. Sustain. Energy Rev.* **2016**, *56*, 1022–1031. [CrossRef]
29. Saada, R.; Kellici, S.; Heil, T.; Morgan, D.; Saha, B. Greener Synthesis of Dimethyl Carbonate Using a Novel Ceria-Zirconia Oxide/Graphene Nanocomposite Catalyst. *Appl. Catal. B Environ.* **2015**, *168–169*, 353–362. [CrossRef]
30. Xuan, K.; Pu, Y.; Li, F.; Luo, J.; Zhao, N.; Xiao, F. Metal-Organic Frameworks MOF-808-X as Highly Efficient Catalysts for Direct Synthesis of Dimethyl Carbonate from CO_2 and Methanol. *Chin. J. Catal.* **2019**, *40*, 553–566. [CrossRef]
31. Honda, M.; Tamura, M.; Nakagawa, Y.; Sonehara, S.; Suzuki, K.; Fujimoto, K.I.; Tomishige, K. Ceria-Catalyzed Conversion of Carbon Dioxide into Dimethyl Carbonate with 2-Cyanopyridine. *ChemSusChem* **2013**, *6*, 1341–1344. [CrossRef] [PubMed]
32. Wang, S.P.; Zhou, J.J.; Zhao, S.Y.; Zhao, Y.J.; Ma, X. Bin Enhancements of Dimethyl Carbonate Synthesis from Methanol and Carbon Dioxide: The In Situ Hydrolysis of 2-Cyanopyridine and Crystal Face Effect of Ceria. *Chin. Chem. Lett.* **2015**, *26*, 1096–1100. [CrossRef]
33. Bansode, A.; Urakawa, A. Continuous DMC Synthesis from CO_2 and Methanol over a CeO_2 Catalyst in a Fixed Bed Reactor in the Presence of a Dehydrating Agent. *ACS Catal.* **2014**, *4*, 3877–3880. [CrossRef]
34. Stoian, D.; Bansode, A.; Medina, F.; Urakawa, A. Catalysis under Microscope: Unraveling the Mechanism of Catalyst de- and Re-Activation in the Continuous Dimethyl Carbonate Synthesis from CO_2 and Methanol in the Presence of a Dehydrating Agent. *Catal. Today* **2017**, *283*, 2–10. [CrossRef]
35. Hong, S.T.; Park, H.S.; Lim, J.S.; Lee, Y.W.; Anpo, M.; Kim, J.D. Synthesis of Dimethyl Carbonate from Methanol and Supercritical Carbon Dioxide. *Res. Chem. Intermed.* **2006**, *32*, 737–747. [CrossRef]
36. Fan, B.; Li, H.; Fan, W.; Zhang, J.; Li, R. Organotin Compounds Immobilized on Mesoporous Silicas as Heterogeneous Catalysts for Direct Synthesis of Dimethyl Carbonate from Methanol and Carbon Dioxide. *Appl. Catal. A Gen.* **2010**, *372*, 94–102. [CrossRef]
37. Tomishige, K.; Kunimori, K. Catalytic and Direct Synthesis of Dimethyl Carbonate Starting from Carbon Dioxide Using CeO_2-ZrO_2 Solid Solution Heterogeneous Catalyst: Effect of H_2O Removal from the Reaction System. *Appl. Catal. A Gen.* **2002**, *237*, 103–109. [CrossRef]
38. Choi, J.C.; Kohno, K.; Ohshima, Y.; Yasuda, H.; Sakakura, T. Tin- or Titanium-Catalyzed Dimethyl Carbonate Synthesis from Carbon Dioxide and Methanol: Large Promotion by a Small Amount of Triflate Salts. *Catal. Commun.* **2008**, *9*, 1630–1633. [CrossRef]
39. Tamboli, A.H.; Chaugule, A.A.; Gosavi, S.W.; Kim, H. $Ce_xZr_{1-x}O_2$ Solid Solutions for Catalytic Synthesis of Dimethyl Carbonate from CO_2: Reaction Mechanism and the Effect of Catalyst Morphology on Catalytic Activity. *Fuel* **2018**, *216*, 245–254. [CrossRef]
40. Reddy, C.V.; Babu, B.; Reddy, I.N.; Shim, J. Synthesis and Characterization of Pure Tetragonal ZrO_2 Nanoparticles with Enhanced Photocatalytic Activity. *Ceram. Int.* **2018**, *44*, 6940–6948. [CrossRef]
41. Zhang, Z.; Wang, R.; Ma, X. Direct Synthesis of DMC from CO_2 and CH_3OH over $Ce_xZr_{1-x-0.1}Y_{0.1}O_2$ Catalysts. *Adv. Mater. Res.* **2011**, *287–290*, 1632–1635. [CrossRef]
42. Zhang, Z.F.; Liu, Z.T.; Liu, Z.W.; Lu, J. DMC Formation over $Ce_{0.5}Zr_{0.5}O_2$ Prepared by Complex-Decomposition Method. *Catal. Lett.* **2009**, *129*, 428–436. [CrossRef]
43. Stoian, D.C.; Taboada, E.; Llorca, J.; Molins, E.; Medina, F.; Segarra, A.M. Boosted CO_2 Reaction with Methanol to Yield Dimethyl Carbonate over Mg–Al Hydrotalcite-Silica Lyogels. *Chem. Commun.* **2013**, *49*, 5489–5491. [CrossRef]
44. Santos, B.A.V.; Silva, V.M.T.M.; Loureiro, J.M.; Rodrigues, A.E. Adsorption of H_2O and Dimethyl Carbonate at High Pressure over Zeolite 3A in Fixed Bed Column. *Ind. Eng. Chem. Res.* **2014**, *53*, 2473–2483. [CrossRef]
45. Lin, C.H.; Lin, S.D.; Yang, Y.H.; Lin, T.P. The Synthesis and Hydrolysis of Dimethyl Acetals Catalyzed by Sulfated Metal Oxides. An Efficient Method for Protecting Carbonyl Groups. *Catal. Lett.* **2001**, *73*, 121–125. [CrossRef]
46. Pluth, M.D.; Bergman, R.G.; Raymond, K.H. Acid Catalysis in Basic Solution: A Supramolecular Host Promotes Orthoformate Hydrolysis. *Science* **2007**, *316*, 85–88. [CrossRef]
47. Zhou, G.; Wang, B.; Cao, R. Acid Catalysis in Confined Channels of Metal-Organic Frameworks: Boosting Orthoformate Hydrolysis in Basic Solutions. *J. Am. Chem. Soc.* **2020**, *142*, 14848–14853. [CrossRef]
48. Lotero, E.; Liu, Y.; Lopez, D.E.; Suwannakarn, K.; Bruce, D.A.; Goodwin, J.G. Synthesis of Biodiesel via Acid Catalysis. *Ind. Eng. Chem. Res.* **2005**, *44*, 5353–5363. [CrossRef]
49. Sasidharan, M.; Kumar, R. Transesterification over Various Zeolites under Liquid-Phase Conditions. *J. Mol. Catal. A Chem.* **2004**, *210*, 93–98. [CrossRef]
50. Hunger, J.; Beta, I.A.; Böhlig, H.; Ling, C.; Jobic, H.; Hunger, B. Adsorption Structures of Water in NaX Studied by DRIFT Spectroscopy and Neutron Powder Diffraction. *J. Phys. Chem. B* **2006**, *110*, 342–353. [CrossRef]
51. Joos, L.; Swisher, J.A.; Smit, B. Molecular Simulation Study of the Competitive Adsorption of H_2O and CO_2 in Zeolite 13X. *Langmuir* **2013**, *29*, 15936–15942. [CrossRef] [PubMed]

52. Fu, Y.; Zhu, H.; Shen, J. Thermal Decomposition of Dimethoxymethane and Dimethyl Carbonate Catalyzed by Solid Acids and Bases. *Thermochim. Acta* **2005**, *434*, 88–92. [CrossRef]
53. Paul, S.; Heyte, S.; Katryniok, B.; Garcia-Sancho, C.; Maireles-Torres, P.; Dumeignil, F. REALCAT: A New Platform to Bring Catalysis to the Lightspeed. *Oil Gas Sci. Technol.–Rev. IFP Energ. Nouv.* **2015**, *70*, 455–462. [CrossRef]